International Journal of Pharmaceutics 479 (2015) 374–380

Contents lists available at ScienceDirect

International Journal of Pharmaceutics

journal homepage: www.elsevier.com/locate/ijpharm

Pharmaceutical nanotechnology

Intravenous delivery of camptothecin-loaded PLGA nanoparticles for the treatment of intracranial glioma

Kyle T. Householder [a,b], Danielle M. DiPerna [a], Eugene P. Chung [a,b], Gregory M. Wohlleb [a,b], Harshil D. Dhruv [c], Michael E. Berens [c], Rachael W. Sirianni [a,b,*]

[a] Barrow Brain Tumor Research Center, Barrow Neurological Institute, 350 W. Thomas Rd., Phoenix, AZ 85013, USA
[b] School of Biological and Health Systems Engineering, Ira A. Fulton Schools of Engineering, Arizona State University, P.O. Box 879709, Tempe, AZ 85287, USA
[c] Cancer and Cell Biology Division, Translational Genomics Research Institute, 455 N. Fifth St., Phoenix, AZ 85004, USA

ARTICLE INFO

Article history:
Received 11 October 2014
Received in revised form 12 December 2014
Accepted 1 January 2015
Available online 3 January 2015

Keywords:
Glioblastoma
Nanoparticles
PLGA
Camptothecin
GL261
Intracranial

ABSTRACT

Effective treatment of glioblastoma multiforme remains a major clinical challenge, due in part to the difficulty of delivering chemotherapeutics across the blood–brain barrier. Systemically administered drugs are often poorly bioavailable in the brain, and drug efficacy within the central nervous system can be limited by peripheral toxicity. Here, we investigate the ability of systemically administered poly (lactic-*co*-glycolic acid) nanoparticles (PLGA NPs) to deliver hydrophobic payloads to intracranial glioma. Hydrophobic payload encapsulated within PLGA NPs accumulated at ~10× higher levels in tumor compared to healthy brain. Tolerability of the chemotherapeutic camptothecin (CPT) was improved by encapsulation, enabling safe administration of up to 20 mg/kg drug when encapsulated within NPs. Immunohistochemistry staining for γ-H2AFX, a marker for double-strand breaks, demonstrated higher levels of drug activity in tumors treated with CPT-loaded NPs compared to free drug. CPT-loaded NPs were effective in slowing the growth of intracranial GL261 tumors in immune competent C57 albino mice, providing a significant survival benefit compared to mice receiving saline, free CPT or low dose CPT NPs (median survival of 36.5 days compared to 28, 32, 33.5 days respectively). In sum, these data demonstrate the feasibility of treating intracranial glioma with systemically administered nanoparticles loaded with the otherwise ineffective chemotherapeutic CPT.

1. Introduction

Malignant gliomas are the most common form of primary brain tumors, afflicting as many as 12,000 patients per year in the United States (Friedman et al., 2000; Grossman and Batara, 2004). Glioblastoma multiforme (GBM) tumors, a grade IV astrocytoma, are distinguished by their fast growing and infiltrative nature. Even after aggressive treatment, which includes tumor resection, radiation, and chemotherapy, the median survival for patients diagnosed with GBM is only 12–14 months (Yang et al., 2014), and few new treatments have advanced to the clinic in the past three decades.

One major challenge to achieving better treatment of GBM is the difficulty of delivering drugs across the blood–brain barrier (BBB), a network of endothelial cells that present both active and passive barriers to the uptake of systemically delivered agents. Chemotherapeutics capable of crossing the BBB are typically poorly soluble and may clear rapidly, and thus high systemic doses are needed to achieve efficacy. This large systemic dose can often have severe toxic effects on peripheral tissue and organs before a treatment benefit is observed.

Thus, many drugs that could be of interest for treating GBM cannot be delivered in doses that are both effective and safe. For example, camptothecin (CPT), a potent DNA damaging chemotherapeutic, is effective at killing cells *in vitro*, but failed in clinical trials due to dose-limiting toxicities and, ultimately, poor efficacy. CPT is rapidly hydrolyzed at physiological pH from its active lactone form to a 10-fold less active, more toxic carboxylate form, which is cleared rapidly once bound to plasma proteins (Mross et al., 2004).

Encapsulation of therapeutics such as CPT in polymeric or liposomal nanoparticles is one strategy that could be used to improve drug action. Drug that has been encapsulated is effectively solubilized and protected from degradation, which prolongs circulation time and increases bioavailability. For example, poly

* Corresponding author at: Neuroscience Research Center, NRC 436, 350 W Thomas Rd., Phoenix, AZ 85013, USA. Tel.: +1 602 406 4493; fax: +1 602 406 7172.
E-mail address: rachael.sirianni@dignityhealth.org (R.W. Sirianni).

http://dx.doi.org/10.1016/j.ijpharm.2015.01.002

(lactic-*co*-glycolic acid) (PLGA) is a biocompatible and biodegradable polymer that can be formed into nanoparticles for encapsulation and sustained release of drug payloads. PLGA nanoparticles are capable of encapsulating a wide range of active agents for sustained release in biological environments, including CPT (Dawidczyk et al., 2014; Dinarvand et al., 2011; Tosi et al., 2013). CPT potency is improved by encapsulation and sustained release when infused directly into tumors (Cirpanli et al., 2010; Sawyer et al., 2011). However, the question of whether CPT-loaded PLGA nanoparticles are capable of treating tumors within the brain when administered intravenously remains unanswered.

The goal of this work was to evaluate the ability of systemically administered CPT-loaded PLGA NPs to treat intracranial GBM in mice. GL261 is a syngeneic mouse glioma cell line that mimics many of the proliferative, invasive, and diffuse characteristics of human GBM (Jacobs et al., 2011; Newcomb and Zagzag, 2009). The use of luciferase expressing GL261 cells (GL261-luc2) allows us to track tumor growth *in vivo* with bioluminescence and, therefore, NP efficacy in immune-competent C57BL/6 albino mice. Nanoparticles were administered to mice bearing orthotopic GL261-luc2 tumors to evaluate specific payload delivery to tumor, peri-tumor, and healthy brain tissue. Efficacy of free CPT versus CPT encapsulated at two doses was determined by tumor growth and survival to test the hypothesis that encapsulation of chemotherapeutic in a nanoparticle could improve systemic therapy of orthotopic GBM.

2. Materials and methods

Camptothecin (CPT), 1,1′-dioctadecyl-3,3,3′,3′-tetramethylindotricarbocyanine iodide (DiR), dichloromethane (DCM), methanol, dimethyl sulfoxide (DMSO), 10% neutral buffered formalin, E-TOXA-Clean and polyvinyl alcohol (PVA) were all purchased from Sigma–Aldrich (St. Louis, MO, USA). Ester terminated poly (lactic-co-glycolic acid) (PLGA) (50:50; inherent viscosity = 0.59 dL/g) was obtained from Lactel (Birmingham, AL, USA). All water used in nanoparticle fabrication was endotoxin free (<0.0050 EU/ml) purchased from G-biosciences (St. Louis, MO, USA). Dulbecco's modified Eagle medium (DMEM), fetal bovine serum (FBS), 0.25% trypsin-EDTA and geneticin selective antibiotic (G-418) were purchased from Gibco Invitrogen (Carlsbad, CA, USA). Greiner T25 tissue culture flasks with filter cap and Costar 96 well assay plates (black, flat-bottom, non-treated polystyrene) were purchased from VWR International (Radnor, PA, USA). Beetle luciferin, potassium salt was purchased from Promega (Madison, WI, UAS). GL261-luc2 cells were a generous gift from Dr. Adrienne Scheck (Barrow Neurological Institute, Phoenix, AZ, USA).

2.1. Cell culture

GL261-luc2 expressing cells were maintained at 37 °C and 5% CO_2 on T25 tissue cultures flasks in DMEM supplemented with glucose, L-glutamine, 10% FBS and G-418 antibiotic. Cells were detached with 0.25% trypsin-EDTA and counted using a cellometer mini (Nexcelom Bioscience, Lawrence, MA, USA) to obtain a final concentration of 50,000 cells/2 μl for tumor inductions.

2.2. Nanoparticle fabrication

Nanoparticles were fabricated in endotoxin-free conditions. All glassware and centrifuge tubes were soaked overnight in a 1% w/v E-TOXA-Clean solution and glassware was baked at 250 °C for 30 min. Nanoparticles were produced by single emulsion-solvent evaporation (McCall and Sirianni, 2013) with slight modification. Briefly, 100 mg of PLGA and either 625 μg DiR or 8 mg CPT was dissolved in 1 ml of a 4:1 DCM: methanol mixture. The dissolved PLGA was added dropwise into 2 ml of 5% (w/v) PVA under vortexing and probe sonicated (Fisher Scientific Model 705 Sonic Dismembrator, Waltham, MA, USA) on ice in 3, 10-s bursts at 40% amplitude. The resulting emulsion was added to 50 ml of 0.3% PVA, and this solution was stirred for 3 h to evaporate solvent. Nanoparticles were collected by centrifugation for 20 min at 20,000 RCF and the resulting nanoparticle pellet was washed three times with DI water. The final nanoparticle pellet was resuspended in 1 ml endotoxin free water containing 25 mg Trehalose, frozen, lyophilized for 48 h, and stored at −80 °C. Blank nanoparticles were made by the same method as above without the addition of CPT or DiR.

2.3. Particle characterization

2.3.1. Sizing and morphology

To visualize surface morphology, lyophilized nanoparticles were mounted on double-sided carbon tape and sputter coated with gold for 30 s at 40 mA. Samples were imaged on a SEM-XL30 Environmental FEG at 10 kV. Nanoparticle diameters were measured with ImageJ (v. 1.48, NIH) for a minimum of 200 nanoparticles taken from 5 images. The hydrodynamic diameter and zeta potential of nanoparticles were determined at a concentration of 1 mg/ml in water by dynamic light scattering (DLS) using a Delsa Nano C (Beckman Coulter, Pasadena, CA, USA).

2.3.2. Drug loading

Loading of CPT and DiR were determined by fluorescence. Nanoparticles were dissolved in DMSO to a concentration of 5 mg/ml. The nanoparticle solution (40 μl) and DMSO (10 μl) were pipetted into a black flat bottom 96 well plate and read on a fluorescent plate reader at the appropriate wavelengths (EX/EM 370/428 nm or 750/780 nm, for CPT or DiR respectively). Three samples were read with technical triplicates averaged. Control curves were constructed by dissolving blank nanoparticles as described above and spiking with known amounts of drug or dye.

2.3.3. Controlled release

The method for measuring release of CPT from nanoparticles was adapted from a method described previously (Deng et al., 2014). Nanoparticles (150 μg) with or without CPT were suspended in 2 ml of 1× PBS and incubated at 37 °C on a shaker. At regular intervals (0.5, 2, 4, 6, 24 and 48 h) samples were removed and centrifuged for 10 min at 20,000 RCF. The nanoparticle pellet was discarded and 970 μl of the supernatant was removed and added to 30 μl of quantification fluid (DMSO: 1N HCL: 10% SDS). Control curves were constructed by spiking blank particle samples with known quantities of CPT for fluorescent readout by the method described above. Three samples were measured for each time point.

2.4. In vivo studies

Nanoparticle brain distribution and tumor treatment efficacy were examined *in vivo* in a total of 64 C57BL/6 albino mice (Harlan Laboratories, Indianapolis, IN, USA). All procedures and animal care practices were performed in accordance with the Barrow Neurological Institute's Institutional Animal Care and Use Committee.

2.4.1. Tumor inductions

Tumor induction protocol followed the methods established by (Abdelwahab et al., 2011) with some modifications. Mice were anesthetized with an intraperitoneal injection of ketamine (100 mg/kg) and xylazine (10 mg/kg) and mounted on a small animal stereotaxic instrument (Model 900, Kopf Instruments, Tujunga, CA, USA). Animal temperature was maintained using a

circulating water heating pad placed beneath the frame. A sterile surgical field was obtained by three alternating passes of betadine solution and 70% isopropanol over the surgical site. An incision was made down the midline of the scalp to expose the skull and a burr hole was drilled to target the striatum (2 mm lateral and 0.1 mm posterior from bregma). A Hamilton syringe filled with 2 μl of the cell suspension (50 k cells) was lowered to a depth of 3 mm and allowed to equilibrate with tissue for 1 min. The syringe was then withdrawn to a depth of 2.6 mm and the cells were infused over 2 min. The syringe was left in place for 1 min before it was removed to reduce back flow. The incision was closed using staples and a triple antibiotic ointment was applied to the scalp before placing the animal in a clean cage over a heating pad to recover. All animals received a single subcutaneous (SQ) injection of buprenorphine (0.1 mg/kg). Ibuprofen was provided in drinking water for 1 week post-op to control pain.

2.4.2. Tumor growth

Tumor growth was monitored every 3–4 days after tumor induction using the Xenogen IVIS Spectrum *in vivo* imaging system (Caliper Life Sciences, Hopkinton, MA, USA). Mice received a SQ injection of 150 mg Luciferin/kg and were imaged under anesthesia (2% isoflurane) at 25 min post injection. Regions of interest (ROIs) were drawn by hand to measure total flux (photons/s) using the IVIS Living Image software.

2.4.3. Tumor localization of particles

25 tumor bearing C57BL/6 albino mice were used to measure accumulation of payload in tumor, peri-tumor and healthy brain tissue. Mice were imaged on the IVIS system one day prior to injection to determine tumor size. On days 4, 8, 12, 16 or 20, mice (n = 5/day) were injected with DiR-loaded nanoparticles (180 mg/kg) in 0.2 mL by tail vein. 2 h post-injection, a blood sample was collected by cardiac puncture before mice were sacrificed and the brain removed, rinsed, and stored at −80 °C. Frozen brains were sliced into 2 mm thick sections and imaged on a LI-COR Odyssey CLx (LI-COR Biosciences, Lincoln, NE, USA). After slices were imaged, 2 mm diameter punches were taken from tumor, peri-tumor and healthy (contralateral) striatal regions. The tissue punches were probe sonicated in 2.5% w/v water for 2, 10 s bursts (40% amplitude). Tissue homogenates (50 μl) were mixed with DMSO (10 μl) in triplicate in a 96 well plate for fluorescent readout (EX/EM 750/780 nm). Control curves were constructed by processing punches from tumor bearing mice that did not receive nanoparticles (n = 8 mice) and spiking with known amounts of DiR.

2.4.4. Tumor treatment efficacy

The antitumor efficacy of CPT-loaded PLGA nanoparticles was tested in 31 C57BL/6 albino mice bearing orthotopic GL261-luc2 tumors. Animals were randomized into four treatment groups: saline, free CPT (10 mg/kg CPT), nanoparticle-encapsulated CPT at a low dose (10 mg/kg CPT) (NP-10), and nanoparticle-encapsulated CPT at a high dose (20 mg/kg CPT) (NP-20). Free CPT was prepared for injection by dissolving CPT (50 mg/ml) in 1 M NaOH and titrating the pH to ~7 with PBS for a final solution of 1 mg/ml CPT. Nanoparticles were prepared for injection by resuspension in sterile saline, and sonicated for 10 min to ensure no aggregates remained (Fisher Scientific Model FS30). Treatments were administered intravenously (IV) by tail vein injection on days 8, 15 and 22 after tumor induction. Treatment efficacy was determined by tumor growth measured by IVIS, as described in Section 2.4.2, every 3–4 days following tumor induction and differences in mean survival time. Mice were monitored daily and euthanized upon >15% weight loss or signs of neurological symptoms.

2.4.5. Camptothecin activity

CPT activity *in vivo* was evaluated using immunohistochemistry (IHC). C57BL/6 albino mice bearing orthotopic GL261-luc2 tumors received an injection of saline, free CPT or NP-20 and were euthanized 2 h after treatment by cardiac perfusion with heparinized saline followed by 10% buffered formalin. Animal brains from each treatment group were harvested for tissue analysis. Formalin fixed brains were sliced into thick sections and embedded in paraffin. H&E staining and IHC staining were performed as described previously (Dhruv et al., 2013). Briefly, 5 μM thick sections from the tissue blocks were baked at 65 °C for 1 h, deparaffinized in three xylene washes, dehydrated in series graded ethanol, and rehydrated in water. Each slide was blocked in blocking buffer (3% goat serum, 1% BSA in PBS) and antigens were retrieved using a sodium citrate buffer (pH 6.5) for 20 min (BondMax Autostainer; Vision Biosystems, Norwell, MA).

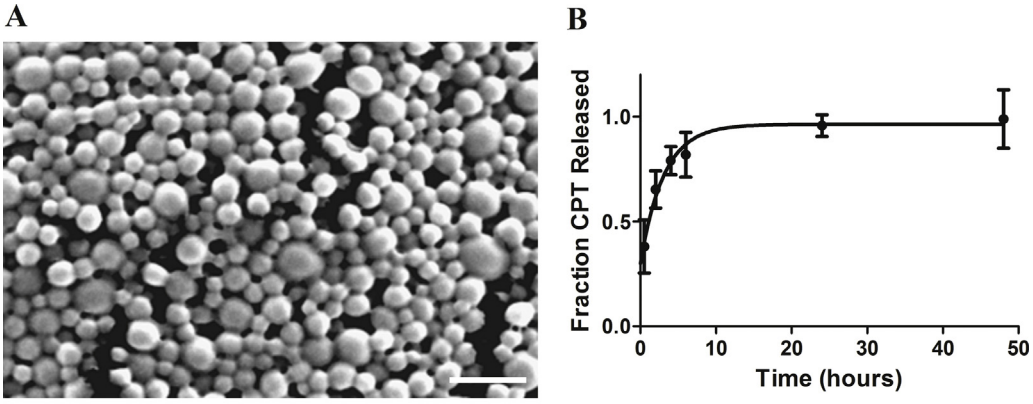

C

Nanoparticles	SEM Diameter (nm)	DLS Diameter (nm)	Zeta Potential (mV)	Loading (%)
PLGA-CPT	123 ± 31	206 ± 32	-21.1	9.6
PLGA-DiR	119 ± 37	204 ± 41	-23.7	0.5

Fig. 1. (A) Representative SEM image of CPT-loaded PLGA nanoparticles. (B) CPT was released from nanoparticles into buffer, with ~80% of total drug released after 6 h. Points and error bars represent the mean ± SD, with 3 samples measured for each time point. (C) CPT- and DiR-loaded nanoparticles had similar diameters, as measured by SEM and DLS, and similar surface charges. (Scale bar = 500 μm).

IHC staining for γH2A.X (#9718, Cell Signaling Technology) and CD31 (ab28364, Abcam) was performed on serial sections from tissue blocks. Slides were incubated with primary antibodies, rinsed, and incubated with a HRP-conjugated secondary antibody for 30 min followed by a DAB substrate. Lastly, sections were counterstained with hematoxylin and coverslipped.

2.5. Statistics

All data analysis was performed in GraphPad Prism 5 software. Brain distribution data were evaluated by a 2-way ANOVA followed by Bonferroni post-test. Tumor growth curves were evaluated by fitting the growth data with a first-order exponential and comparing tumor doubling times using an ANOVA followed by Tukey's multiple comparison test. Survival differences were evaluated from the Kaplan–Meier plot with the Mantel–Cox test. Differences were considered statistically significant for an alpha level of 0.05.

3. Results

3.1. Nanoparticle characterization

SEM analysis confirmed that nanoparticles possessed a spherical shape with smooth surface morphology (Fig. 1A, Supplementary Fig. 1). Nanoparticles sizes were relatively monodisperse (Fig. 1(A and C)) with a mean particle diameter of 123 ± 31 and 119 ± 37 nm for CPT and DiR nanoparticles, respectively, as measured by SEM. DLS measurements yielded hydrodynamic diameters of 206 ± 32 and 204 ± 41 nm respectively and zeta potentials of -21.1 and -23.7 mV for CPT and DiR loaded nanoparticles, respectively (Fig. 1C). Hydrophobic agents were effectively encapsulated in the NPs with drug loading efficiency of 9.6% for CPT and 0.5% for DiR. The CPT release profile of the particles was determined *in vitro* in PBS at 37 °C (Fig. 1B). Drug was initially released from nanoparticles in a burst of ~80% over 6 h, and complete CPT release was observed within 24 h.

Supplementry material related to this article found, in the online version, at http://dx.doi.org/10.1016/j.ijpharm.2015.01.002.

3.2. In vivo studies

3.2.1. Tumor localization

NPs loaded with DiR, a hydrophobic, near infrared dye shown to release less than 5% in 24 h and commonly used to track NPs (Lu et al., 2014; Yao et al., 2014), were administered IV to evaluate the ability of NPs to deliver hydrophobic payload to intracranial GL261-luc2 tumors. Biopsy punches were taken from the tumor core, peri-tumor region below the tumor, and contralateral (healthy) hemisphere (Fig. 2A). Nanoparticle payload accumulated in the tumor core at significantly higher concentrations compared to both healthy and peri-tumor brain regions ($p < 0.05$) at day 12, 16 and 20 (Fig. 2B). Payload delivery was positively correlated to tumor size for both tumor core and peri-tumor regions ($p = 0.0002$ and 0.048, respectively) (Fig. 2C).

3.2.2. Tumor treatment efficacy

The tolerability and efficacy of CPT delivered in nanoparticle-encapsulated versus free form were evaluated in C57BL/6 albino mice bearing intracranial GL261-luc2 tumors. Subjects received weekly injections of saline, free CPT, NP-10, or NP-20 for 3 cycles. Subjects that received nanoparticle encapsulated CPT at both low and high dose experienced similar weight loss following treatment when compared to free CPT (Fig. 3A, shown with error bars in Supplementary Fig. 2). Tumor growth in saline-treated subjects was exponential, and no significant differences in tumor size were

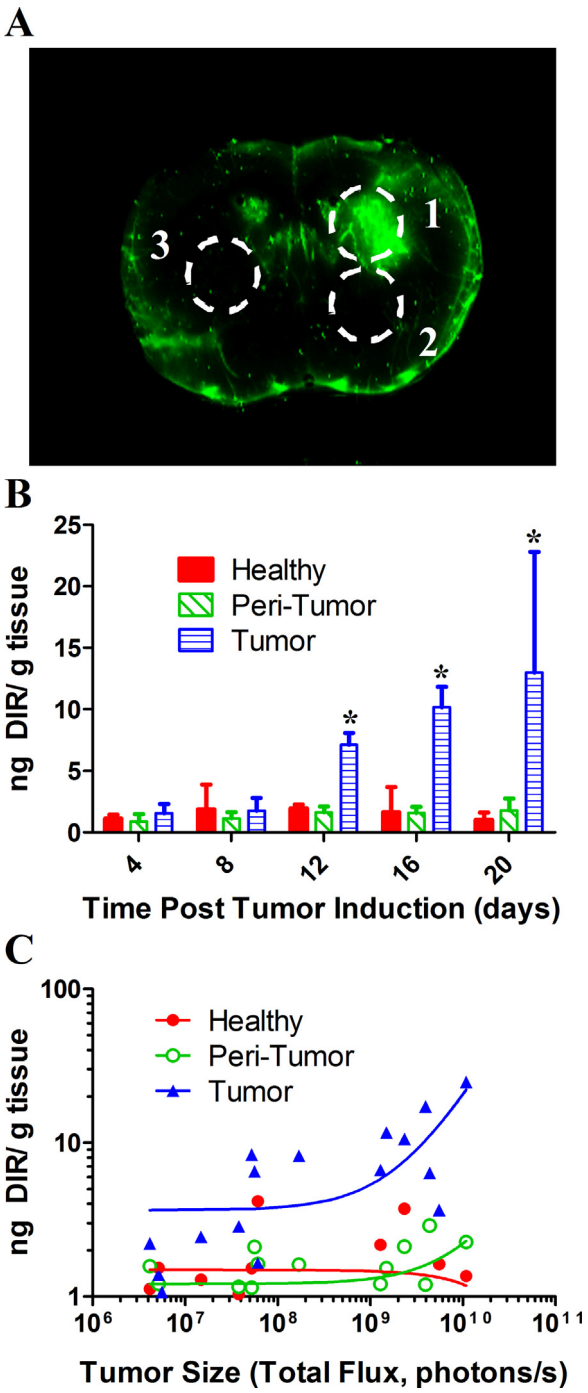

Fig. 2. (A) DiR distribution (green) in a tumor bearing mouse brain captured on the LI-COR Oddyssey. Regions marked indicate example tissue punch locations used for tumor (1), peri-tumor (2) and healthy brain (3). (B) DiR accumulation was significantly higher in the tumor compared to peri-tumor or healthy brain regions, 12, 16 and 20 days post tumor implantation ($p = 0.01$) Bars indicate mean ±SD ($n = 5$ mice/day). (C) The amount of DiR/g tissue, quantified by fluorescence for each region, positively correlated with tumor size for both tumor core and peri-tumor regions ($p = 0.002$ and 0.048, respectively).

observed for mice treated with free CPT or NP-10 (Fig. 3B). However, tumor growth was significantly slowed by treatment with NP-20. Additionally, NP-20 provided a significant survival benefit over the other treatment groups with a median survival of 36.5 days compared to 28, 32 and 33.5 days for saline, free CPT and NP-10 respectively (Fig. 3C). In a separate series of experiments, we established that blank nanoparticles did not alter survival when compared to saline treated controls (Supplementary Fig. 3).

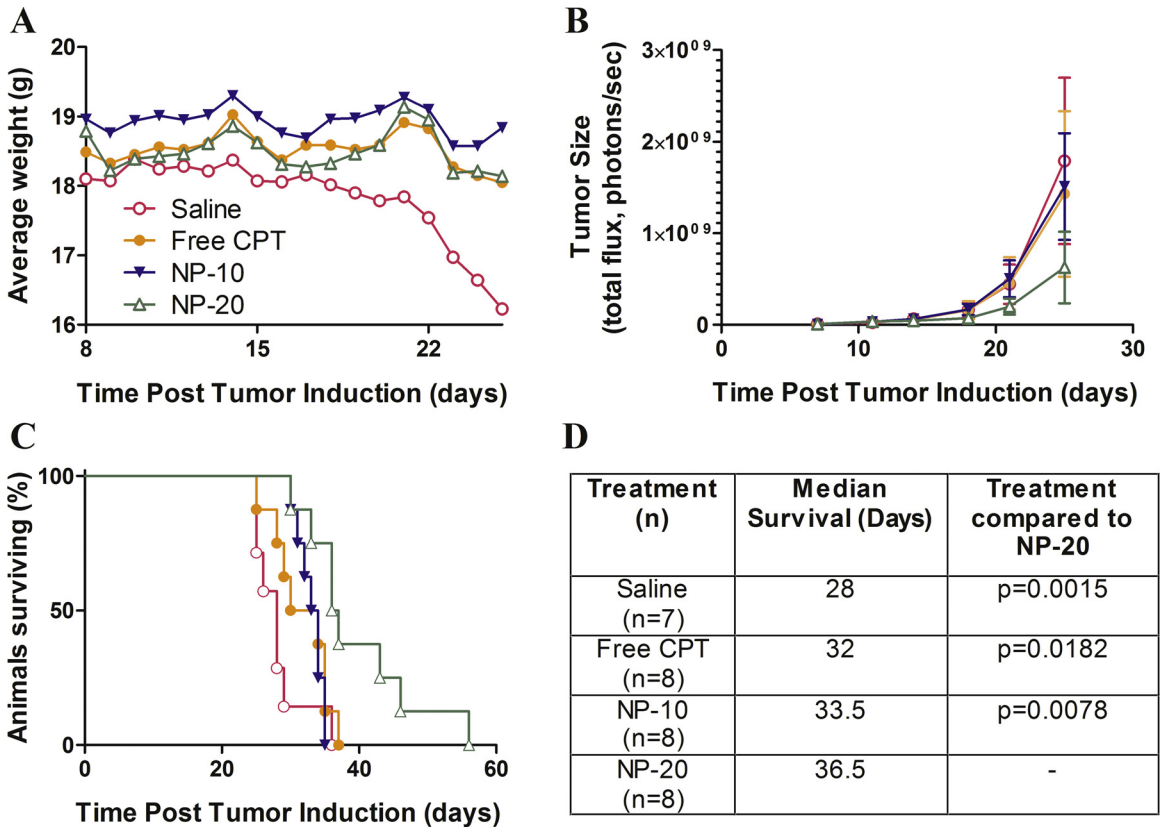

Treatment (n)	Median Survival (Days)	Treatment compared to NP-20
Saline (n=7)	28	p=0.0015
Free CPT (n=8)	32	p=0.0182
NP-10 (n=8)	33.5	p=0.0078
NP-20 (n=8)	36.5	-

Fig. 3. (A) Mice receiving CPT either freely or in a NP showed similar weight fluctuations over the course of treatments. Saline treated mice weight remained steady until the tumor burden became too great. (B) Tumor burden monitored by IVIS showed NP-20 significantly slowed tumor growth ($p = 0.01$) and provided a significant survival benefit (C and D) compared to all other treatments. Error bars indicate ± SD.

Supplementry material related to this article found, in the online version, at http://dx.doi.org/10.1016/j.ijpharm.2015.01.002.

3.2.3. Camptothecin activity

CPT bioactivity was examined by γH2A.X staining in intracranial tumors of animals treated with saline, free CPT, and nanoparticle encapsulated CPT (Fig. 4). Tumor sections taken from NP-20 treated mice showed an increase in staining intensity of γH2A.X compared to free CPT, with an average score of 3.0 as compared to 2.0, respectively (blinded scoring performed by board certified pathologist). These data support the hypothesis that encapsulation of CPT in nanoparticles allows for the delivery of greater amounts of CPT without adverse effects (Fig. 4). To rule out the possibility that higher delivery of nanoparticle encapsulated CPT was due to higher vascularity of those particular subjects, we also examined CD31 staining intensity across different treatment groups (Fox et al., 1993). Each treatment group showed similar CD31 staining intensity.

4. Discussion

This study presents the use of CPT-loaded PLGA NPs for the systemic treatment of an orthotopic murine glioma. We achieved a loading of CPT in our nanoparticles of ∼10% by weight; this value is higher than our theoretical loading of 8%, indicating that more PLGA was lost than CPT during the nanoparticle fabrication process. Loss of PLGA during nanoparticle fabrication has been reported previously (Sawyer et al., 2011), and our loading is consistent with the 5–25% loading reported by other groups encapsulating CPT in PLGA (Deng et al., 2014; McCarron et al., 2008). The average hydrated nanoparticle diameter measured by DLS (∼200 nm) was larger than the diameter measured by SEM (∼120 nm), which is expected, given that NPs will become hydrated in the aqueous environment required for DLS and that a fraction of nanoparticles will experience aggregation after resuspension. The zeta potential of our nanoparticles was approximately −21 mV, which is more negative than the purposed optimal range of −10 to +10 mV required to minimize nonspecific nanoparticle interactions and MPS cell clearance (Davis, 2009). NPs displayed CPT release kinetics typically observed for PLGA nanoparticles, with an initial, rapid burst release followed by a period of slowed release and the majority of drug being released within several days. Drug was therefore effectively encapsulated for subsequent release in physiological environments.

One advantage of using PLGA nanoparticles as drug delivery vehicles is that encapsulation of hydrophobic agents can improve their solubility and reduce toxicity. Toxicity remains a problem for CPT, which has a literature reported maximum tolerated dose (MTD) of 8–10 mg/kg (Han and Davis, 2013). In our hands, injection of free CPT at a dose of 16 mg/kg caused almost instant death (5–10 s), presumably due to its poor solubility. However, CPT was well-tolerated when encapsulated in PLGA NPs; no signs of acute drug toxicity were observed for doses of up to 30 mg/kg. We observed an MTD for PLGA-CPT NPs of 20 mg/kg CPT, with higher doses resulting in weight loss after treatment (data not shown). This increase in CPT tolerability could be due to a combination of increased solubility and reduction of peak dose due to prolonged release of CPT from the particles. The extended release profile seen could also increase tolerability by allowing particles to deliver CPT to the tumor or be cleared before a majority of the CPT is released, thereby reducing CPT exposure to healthy cells.

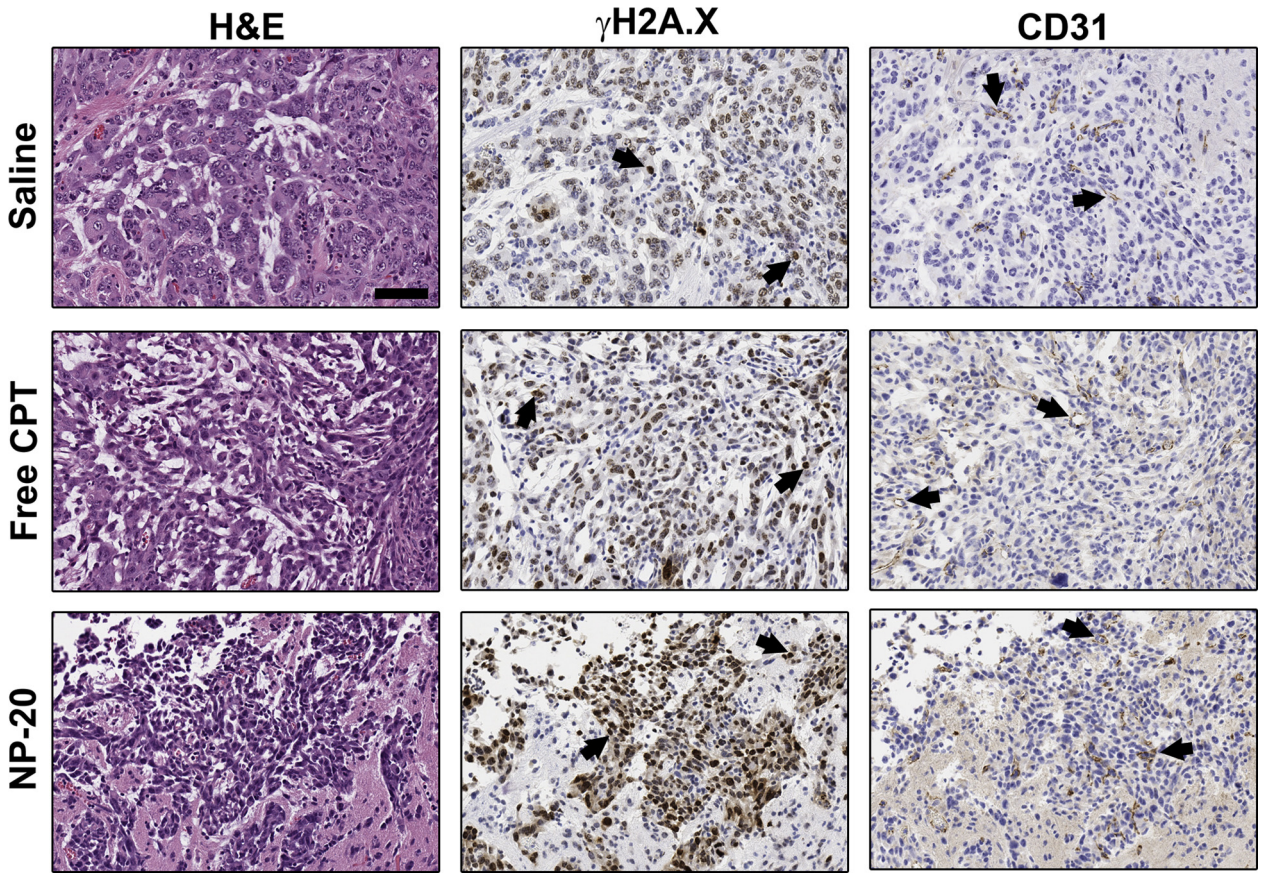

Fig. 4. Left panel shows H&E staining of the tumor cells in saline, free CPT and nanoparticle encapsulated CPT (20 mg/Kg) treated animals. Center panel shows γH2A.X staining on the serial section, and demonstrates very high γH2A.X staining for animals treated with nanoparticle encapsulated CPT (20 mg/Kg) (IHC score = 3) as compared to saline (IHC score = 1–2) and free CPT (IHC score = 2) treated animals. Right panel shows the CD31 staining on the serial section, and demonstrates similar staining intensity in all the treatment group. Positive staining in each section is indicated by black arrow. All the images are taken at 20× magnification (scale bar in top left panel = 100 μm). (n = 3 mice/treatment).

The difficulty of delivering drugs across the BBB makes the use of an intracranial tumor model critical for evaluating nanoparticle drug delivery; however, the most common GBM models (i.e. U87, U118, 9L) grow as bulky tumors, with well-defined borders and a highly disrupted BBB (Jacobs et al., 2011; Newcomb and Zagzag, 2009). The GL261 tumor model was chosen for this work for several reasons. First, human GBM is characterized by diffuse and highly infiltrative growth, and it has been shown that GL261 tumors better recapitulate these characteristics with tumor cells invading into surrounding brain parenchyma where the BBB is still intact (Seligman et al., 1939; Szatmári et al., 2006). Additionally, GL261 cells share key genomic features with human GBM, including activated K-ras (mutant) and mutant p53, along with increased activation of the PI3K/Akt pathway (Jacobs et al., 2011; Oh et al., 2014). Here we utilized a luc2 transfected GL261 model, which has been shown to have the same growth characteristics *in vivo* as the parent cell line, while enabling noninvasive tracking of tumor growth over time (Abdelwahab et al., 2011; Clark et al., 2014). In future work, this model could be used to evaluate the delivery of molecularly targeted drugs that would not otherwise cross the BBB.

It is well-established that nanoparticles can extravasate from peripheral circulation through leaky tumor vasculature into tumor core, a phenomenon termed the enhanced permeation and retention (EPR) effect; however, the optimal nanoparticle size for achieving the greatest EPR effect will depend on a number of factors including tumor type, location, and size of tumor. EPR data has been reported for nanoparticles ranging from 20–1000 nm in various tumor models (Acharya and Sahoo, 2011; Fang et al., 2011; Greish, 2010; Prabhakar et al., 2013). Previously, 10 nm DSPE-PEG micelles have been shown to passively accumulate in intracranial GL261 tumors; however, to our knowledge, the nanoparticle size requirement for EPR-mediated delivery to intracranial GL261 tumors has not been evaluated. Thus, we were interested to study how nanoparticle payload was delivered selectively to tumor core versus periphery during tumor progression. Biopsy punches taken from the brains of tumor bearing mice administered PLGA-DiR NPs demonstrated that NPs preferentially accumulate in the tumor core, and this preferential delivery increased as a function of tumor size and with time post-tumor induction. These data suggest that effective delivery of hydrophobic payloads can be achieved even in late stages of growth in this intracranial model.

The growth of intracranial GL261-luc2 tumors was unaffected by treatment with free drug or with encapsulated drug at the MTD for free drug of 10 mg/kg. However, CPT-loaded PLGA nanoparticles delivered systemically at a dose of 20 mg/kg CPT slowed tumor growth and produced a significant increase in survival compared to all other treatments. CPT is a potent DNA damaging therapy and acts on cells by inhibiting enzyme DNA topoisomerase I, which leads to generation of DNA double strand breaks (DSB), leading to apoptosis. DSB activates the DNA damage response (DDR) and produces accumulation of phosphorylated histone H2A.X (γH2A.X), a hallmark of DDR (Furuta et al., 2003). IHC analysis of γH2A.X validates that the slowed tumor growth and significant increase in survival of animals treated with NP-20 was due to the enhanced tolerability of nanoparticle encapsulated CPT, which enabled a higher total dose to be delivered.

PLGA is both biocompatible and biodegradable, and has been used extensively for improving the action of chemotherapeutics (Dawidczyk et al., 2014; Dinarvand et al., 2011; Gu et al., 2013; Guo et al., 2013; Tosi et al., 2013), including in humans. For example, PLA-PEG nanoparticles encapsulating the chemotherapeutic drug doxorubicin are the subject of a phase II clinical trial in prostate cancer and non-small cell lung carcinoma (Hrkach et al., 2012). Other groups have encapsulated CPT within PLGA nanoparticles, and these formulations were effective when delivered directly to intracranial tumors, either by convection enhance delivery or from inside a hydrogel implant (Cirpanli et al., 2010; Sawyer et al., 2011). The data presented here confirm that encapsulation of CPT can improve its activity. To our knowledge, this study is the first to report effective therapy of an intracranial tumor by systemic administration of CPT-loaded PLGA nanoparticles. Surface modification of nanoparticles – for example, attachment of poly (ethylene glycol) to improve circulation time, or ligands designed to facilitate transport of nanoparticles across the BBB could further improve payload delivery to the CNS (McCall et al., 2014). Enhancing delivery across an intact BBB to provide pan-CNS delivery of chemotherapies will improve drug access to invading cancer cells to improve tumor therapy.

Conflicts of interest

The authors have no conflicts of interest to declare.

Acknowledgements

We gratefully acknowledge funding from the Ben and Catherine Ivy Foundation and Barrow Neurological Foundation. The authors would like to thank Dr. Shipra Garg (Board Certified pathologist) for IHC scoring, Dr. Vikram Kodibagkar (Arizona State University) for use of DLS equipment and the LeRoy Eyring Center for Solid State Science at Arizona State University for use of SEM facilities.

References

Abdelwahab, M.G., Sankar, T., Preul, M.C., Scheck, A.C., 2011. Intracranial Implantation with subsequent 3D in vivo bioluminescent imaging of murine gliomas. J. Vis. Exp. doi:http://dx.doi.org/10.3791/3403.

Acharya, S., Sahoo, S.K., 2011. PLGA nanoparticles containing various anticancer agents and tumour delivery by EPR effect. Adv. Drug Deliv. Rev. 63, 170–183. doi:http://dx.doi.org/10.1016/j.addr.2010.10.008 EPR effect based drug design and clinical outlook for enhanced cancer chemotherapy.

Cirpanli, Y., Bilensoy, E., Dogan, A.L., Calis, S., 2010. Development of polymeric and cyclodextrin nanoparticles for camptothecin delivery. J. Controlled Release 148, e21–e23. doi:http://dx.doi.org/10.1016/j.jconrel.2010.07.034 11th European Sumposium on Controlled Drug Delivery.

Clark, A.J., Safaee, M., Oh, T., Ivan, M.E., Parimi, V., Hashizume, R., Ozawa, T., James, C. D., Bloch, O., Parsa, A.T., 2014. Stable luciferase expression does not alter immunologic or in vivo growth properties of GL261 murine glioma cells. J. Transl Med. 12. doi:http://dx.doi.org/10.1186/s12967-014-0345-4.

Davis, M.E., 2009. The first targeted delivery of siRNA in humans via a self-assembling, cyclodextrin polymer-based nanoparticle: from concept to clinic. Mol Pharm. 6, 659–668. doi:http://dx.doi.org/10.1021/mp900015y.

Dawidczyk, C.M., Russell, L.M., Searson, P.C., 2014. Nanomedicines for cancer therapy: state-of-the-art and limitations to pre-clinical studies that hinder future developments. Chem. Eng. 2, 69. doi:http://dx.doi.org/10.3389/fchem.2014.00069.

Deng, Y., Saucier-Sawyer, J.K., Hoimes, C.J., Zhang, J., Seo, Y.-E., Andrejecsk, J.W., Saltzman, W.M., 2014. The effect of hyperbranched polyglycerol coatings on drug delivery using degradable polymer nanoparticles. Biomaterials 35, 6595–6602. doi:http://dx.doi.org/10.1016/j.biomaterials.2014.04.038.

Dhruv, H.D., McDonough Winslow, W.S., Armstrong, B., Tuncali, S., Eschbacher, J., Kislin, K., Loftus, J.C., Tran, N.L., Berens, M.E., 2013. Reciprocal activation of transcription factors underlies the dichotomy between proliferation and invasion of glioma cells. PLoS ONE 8, e72134. doi:http://dx.doi.org/10.1371/journal.pone.0072134.

Dinarvand, R., Sepehri, N., Manoochehri, S., Rouhani, H., Atyabi, F., 2011. Polylactide-*co*-glycolide nanoparticles for controlled delivery of anticancer agents. Int. J. Nanomedicine 6, 877–895. doi:http://dx.doi.org/10.2147/IJN.S18905.

Fang, J., Nakamura, H., Maeda, H., 2011. The EPR effect: unique features of tumor blood vessels for drug delivery, factors involved, and limitations and augmentation of the effect. Adv. Drug Deliv. Rev. 63, 136–151. doi:http://dx.doi.org/10.1016/j.addr.2010.04.009 EPR effect based drug design and clinical outlook for enhanced cancer chemotherapy.

Fox, S.B., Gatter, K.C., Bicknell, R., Going, J.J., Stanton, P., Cooke, T.G., Harris, A.L., 1993. Relationship of endothelial cell proliferation to tumor vascularity in human breast cancer. Cancer Res. 53, 4161–4163.

Friedman, H.S., Kerby, T., Calvert, H., 2000. Temozolomide and treatment of malignant glioma. Clin. Cancer Res. Off. J. Am. Assoc. Cancer Res. 6, 2585–2597.

Furuta, T., Takemura, H., Liao, Z.-Y., Aune, G.J., Redon, C., Sedelnikova, O.A., Pilch, D.R., Rogakou, E.P., Celeste, A., Chen, H.T., Nussenzweig, A., Aladjem, M.I., Bonner, W. M., Pommier, Y., 2003. Phosphorylation of histone H2AX and activation of Mre11, Rad50, and Nbs1 in response to replication-dependent DNA double-strand breaks induced by mammalian DNA topoisomerase I cleavage complexes. J. Biol. Chem. 278 (20), 303–20312. doi:http://dx.doi.org/10.1074/jbcM300198200.

Greish, K., 2010. Enhanced permeability and retention (EPR) effect for anticancer nanomedicine drug targeting. In: Grobmyer, S.R., Moudgil, B.M. (Eds.), Cancer Nanotechnology, Methods in Molecular Biology. Humana Press, pp, pp. 25–37.

Grossman, S.A., Batara, J.F., 2004. Current management of glioblastoma multiforme. Semin. Oncol. 31, 635–644. doi:http://dx.doi.org/10.1053/j.seminoncol.2004.07.005 Brain tumors.

Han, H., Davis, M.E., 2013. Single-antibody, targeted nanoparticle delivery of camptothecin. Mol. Pharm. 10, 2558–2567. doi:http://dx.doi.org/10.1021/mp300702x.

Hrkach, J., Hoff, D.V., Ali, M.M., Andrianova, E., Auer, J., Campbell, T., Witt, D.D., Figa, M., Figueiredo, M., Horhota, A., Low, S., McDonnell, K., Peeke, E., Retnarajan, B., Sabnis, A., Schnipper, E., Song, J.J., Song, Y.H., Summa, J., Tompsett, D., Troiano, G., Hoven, T.V.G., Wright, J., LoRusso, P., Kantoff, P.W., Bander, N.H., Sweeney, C., Farokhzad, O.C., Langer, R., Zale, S., 2012. Preclinical development and clinical translation of a PSMA-targeted docetaxel nanoparticle with a differentiated pharmacological profile. Sci. Transl. Med. 4, 128ra39. doi:http://dx.doi.org/10.1126/scitranslmed.3003651.

Jacobs, V.L., Valdes, P.A., Hickey, W.F., De Leo, J.A., 2011. Current review of in vivo GBM rodent models: emphasis on the CNS-1 tumour model. ASN NEURO 3. doi:http://dx.doi.org/10.1042/AN20110014.

Lu, J., Chuan, X., Zhang, H., Dai, W., Wang, X., Wang, X., Zhang, Q., 2014. Free paclitaxel loaded PEGylated-paclitaxel nanoparticles: preparation and comparison with other paclitaxel systems in vitro and in vivo. Int. J. Pharm. 471, 525–535. doi:http://dx.doi.org/10.1016/j.ijpharm.2014.05.032.

McCall, R.L., Sirianni, R.W., 2013. PLGA nanoparticles formed by single- or double-emulsion with vitamin E-TPGS. J. Vis. Exp. doi:http://dx.doi.org/10.3791/51015.

McCall, R.L., Cacaccio, J., Wrabel, E., Schwartz, M.E., Coleman, T.P., Sirianni, R.W., 2014. Pathogen-inspired drug delivery to the central nervous system. Tissue Barriers e944449. doi:http://dx.doi.org/10.4161/21688362.2014.944449.

McCarron, P.A., Marouf, W.M., Quinn, D.J., Fay, F., Burden, R.E., Olwill, S.A., Scott, C.J., 2008. Antibody targeting of camptothecin-loaded PLGA nanoparticles to tumor cells. Bioconjug. Chem. 19, 1561–1569. doi:http://dx.doi.org/10.1021/bc800057g.

Mross, K., Richly, H., Schleucher, N., Korfee, S., Tewes, M., Scheulen, M.E., Seeber, S., Beinert, T., Schweigert, M., Sauer, U., Unger, C., Behringer, D., Brendel, E., Haase, C.G., Voliotis, D., Strumberg, D., 2004. A phase I clinical and pharmacokinetic study of the camptothecin glycoconjugate, BAY 38-3441, as a daily infusion in patients with advanced solid tumors. Ann. Oncol. 15, 1284–1294. doi:http://dx.doi.org/10.1093/annonc/mdh313.

Newcomb, E.W., Zagzag, D., 2009. The murine GL261 glioma experimental model to assess novel brain tumor treatments. In: Meir, E.G. (Ed.), CNS Cancer, Cancer Drug Discovery and Development. Humana Press, pp. 227–241.

Oh, T., Fakurnejad, S., Sayegh, E.T., Clark, A.J., Ivan, M.E., Sun, M.Z., Safaee, M., Bloch, O., James, C.D., Parsa, A.T., 2014. Immunocompetent murine models for the study of glioblastoma immunotherapy. J. Transl. Med. 12, 107. doi:http://dx.doi.org/10.1186/1479–5876-12–107.

Prabhakar, U., Maeda, H., Jain, R.K., Sevick-Muraca, E.M., Zamboni, W., Farokhzad, O. C., Barry, S.T., Gabizon, A., Grodzinski, P., Blakey, D.C., 2013. Challenges and key considerations of the enhanced permeability and retention (EPR) effect for nanomedicine drug delivery in oncology. Cancer Res. 73, 2412–2417. doi:http://dx.doi.org/10.1158/0008-5472CAN-12-4561.

Sawyer, A.J., Saucier-Sawyer, J.K., Booth, C.J., Liu, J., Patel, T., Piepmeier, J.M., Saltzman, W.M., 2011. Convection-enhanced delivery of camptothecin-loaded polymer nanoparticles for treatment of intracranial tumors. Drug Deliv. Transl. Res. 1, 34–42. doi:http://dx.doi.org/10.1007/s13346-010-0001-3.

Seligman, A.M., Shear, M.J., Alexander, L., 1939. Studies in carcinogenesis: VIII. Experimental production of brain tumors in mice with methylcholanthrene. Am. J Cancer 37, 364–395. doi:http://dx.doi.org/10.1158/ajc.1939.364.

Szatmári, T., Lumniczky, K., Désaknai, S., Trajcevski, S., Hídvégi, E.J., Hamada, H., Sáfrány, G., 2006. Detailed characterization of the mouse glioma 261 tumor model for experimental glioblastoma therapy. Cancer Sci. 546–553. doi:http://dx.doi.org/10.1111/j1349–7006.2006.00208.x.

Tosi, G., Bortot, B., Ruozi, B., Dolcetta, D., Vandelli, M.A., Forni, F., Severini, G.M., 2013. Potential use of polymeric nanoparticles for drug delivery across the blood–brain barrier. Curr. Med. Chem. 20, 2212–2225.

Yang, L.-J., Zhou, C.-F., Lin, Z.-X., 2014. Temozolomide and radiotherapy for newly diagnosed glioblastoma multiforme: a systematic review. Cancer Invest. 32, 31–36. doi:http://dx.doi.org/10.3109/07357907.2013.861474.

Yao, J., Li, Y., Sun, X., Dahmani, F.Z., Liu, H., Zhou, J., 2014. Nanoparticle delivery and combination therapy of gambogic acid and all-trans retinoic acid. Int. J. Nanomed. 9, 3313–3324. doi:http://dx.doi.org/10.2147/IJN.S62793.